Available online at www.sciencedirect.com
SCIENCE DIRECT®
Journal of Molecular Catalysis A: Chemical 226 (2005) 263–268
JOURNAL OF MOLECULAR CATALYSIS A: CHEMICAL
www.elsevier.com/locate/molcata

Novel Pd/TiO_2–ZrO_2 catalysts for methane total oxidation at low temperature and their ^{18}O-isotope exchange behavior

W. Lin[a], L. Lin[a], Y.X. Zhu[a,*], Y.C. Xie[a], K. Scheurell[b], E. Kemnitz[b]

[a] *State Key Laboratory for Structural Chemistry of Unstable and Stable Species, College of Chemistry and Molecular Engineering, Peking University, 100871 Beijing, China*
[b] *Institute of Chemistry, Humboldt University, Brook Taylor Str. 2, D-12489 Berlin, Germany*

Received 8 September 2004; received in revised form 28 October 2004; accepted 28 October 2004

Abstract

TiO_2–ZrO_2 binary oxide supported palladium catalysts were prepared and evaluated for the catalytic combustion of methane at low temperature. Although XRD patterns of TiO_2–ZrO_2 binary oxides show individual anatase TiO_2 and monoclinic ZrO_2 peaks without shift, the combination of TiO_2 and ZrO_2 obviously favors the catalytic performance. Catalyst Pd/TiZr2 has activity much higher than Pd/TiO_2, even higher than Pd/ZrO_2, which is one of the most active catalysts for methane combustion. The results of TPR and ^{18}O-isotope exchange experiments demonstrate that the excellent activity of Pd/TiZr2 is due to its high oxygen mobility and moderate reducibility, which is in accordance with our previous work. XPS results indicate that the dispersion of Pd has little influence on the catalytic activity.

Keywords: Methane combustion; Palladium; TiO_2–ZrO_2 binary oxide; Reducibility; Oxygen mobility

1. Introduction

Catalytic total oxidation of methane is an effective way to use methane as an environment-friendly fuel [1–4]. Among the catalysts investigated, supported palladium showed the highest activity for this reaction [5,6], especially ZrO_2-supported catalysts [7–14]. Great efforts have been devoted to the investigation of the reaction mechanism and the metal–support interaction in order to get a deep understanding of the reason for high activity [7–21]. It is generally accepted that the catalytic performance is strongly dependent on the nature of the support, but the key factors influencing the catalytic activity are still in debate. Ciuparu et al. [17–20] found that the support contributed significantly to the oxygen pool of the PdO phase available for the methane combustion and the stabilizing effect of the support for PdO may be related to the oxygen transfer from the support to the PdO particles. Our recent work [22] on $Pd/TiO_2/Al_2O_3$ system proved that the reducibility and oxygen mobility of PdO were two factors directly related to the overall catalytic activity of palladium catalysts. A moderate reducibility and high oxygen mobility will lead to high methane combustion activity.

In order to increase the activity of supported palladium catalyst, various kinds of modified ZrO_2 have been investigated as supports [23–27]. However, among these catalysts ZrO_2 was mostly used as additives, and to our knowledge no palladium catalysts supported on modified ZrO_2 have been reported to be superior to Pd/ZrO_2 until now. On the other hand, titania modification of KIT-1 mesoporous materials [28] or alumina [22,29] supports could improve the methane combustion activity of palladium. Kang et al. [28] reported that titania chemically bonded with the skeleton of mesoporous materials interacted with the co-loaded palladium and suppressed the decomposition of palladium oxide, which was the more active phase in the methane combustion compared to palladium, and consequently leaded to the

* Corresponding author. Tel.: +86 10 62751703; fax: +86 10 62751725.
E-mail address: zhuyx@pku.edu.cn (Y.X. Zhu).

1381-1169/$ – see front matter © 2004 Elsevier B.V. All rights reserved.
doi:10.1016/j.molcata.2004.10.048

improvement of the catalytic performance. Our previous work [22] showed that the addition of titania into alumina enhanced the reduction as well as the oxygen mobility of palladium oxide, hence generated the catalysts with higher activity for low temperature catalytic combustion of methane. In the present paper, palladium catalysts with titania–zirconia complex oxides as supports were prepared and tested for catalytic total oxidation of methane at low temperature. Temperature-programmed reduction (TPR) and temperature-programmed ^{18}O-isotope exchange techniques were employed to investigate the reducibility and oxygen mobility. The results show that Pd/TiZr2 have a moderate reducibility and higher oxygen exchange activity compared to other catalysts, which make it one of the most active catalysts for methane total oxidation at low temperature.

2. Experimental

2.1. Catalyst preparation

TiO_2–ZrO_2 binary oxide was prepared by coprecipitation method. $Ti(C_4H_9O)_4$ and C_2H_5OH were mixed with volume ratio of 1:4. Then the mixture solution and $Zr(NO_3)_4$ solution were dropped simultaneously into 5 mol L^{-1} $NH_3{\cdot}H_2O$ at room temperature. Afterwards, the precipitate was then vacuum filtered and dried at 120 °C followed by calcinations at 500 °C in air for 8 h. Catalysts of 2 wt.% Pd/TiO_2–ZrO_2 were prepared by impregnation method using palladium nitrate as precursor. The catalysts were dried at 120 °C overnight and calcined in air at 500 °C for 4 h.

2.2. Catalytic activity tests

Activity evaluation was carried out in a U-shaped fixed-bed microreactor (i.d. = 10 mm) with a continuous flow at atmospheric pressure. The catalysts were pressed to pellets, and then crushed and sieved to 40–60 mesh. The catalyst (120 mg) was put in the microreactor and pretreated in flowing air at 500 °C for 1 h then cooled down to room temperature before the catalytic test. A K-type thermocouple was fixed to the middle of the catalyst bed to measure the reaction temperature and to control the furnace temperature. The feed gas was 1% CH_4 in air. The total feed flow rate was 66 mL min^{-1}, corresponding to a gas hourly mass velocity (GHMV) of 33,000 mL h^{-1} g^{-1}. The reactants and products were analyzed with an on-line SQ-206 gas chromatogram equipped with hydrogen flame ionization detector (FID). A methanator of nickel catalyst was used to convert CO_2 and CO to CH_4 for FID analysis. A four-meter long Porapak Q column was employed to separate CH_4, CO and CO_2. The peaks of CH_4, CO and CO_2 were collected with a computer and the conversion of methane was calculated automatically. Methane conversion was measured from 275 to 500 °C at an interval of 25 °C. Each reaction temperature was kept stable for 30 min before analyzing the effluent gas. The temperatures corresponding to 10, 50, and 90% methane conversion, $T_{10\%}$, $T_{50\%}$, and $T_{90\%}$, were obtained from the temperature dependent plot of methane conversion.

2.3. Characterization techniques

Surface area was determined by using BET method based on N_2 adsorption with a Micromeritics ASAP 2010 Analyzer. The samples were degassed in vacuum (10^{-3} Pa) for 2 h at 300 °C prior to adsorption measurements.

Phase composition of the catalysts was determined with a Rigaku D/MAX-200 X-ray powder diffractometer with Ni-filtered Cu Kα radiation at 40 kV and 100 mA.

Surface composition of the samples was measured by using a Kratos Axis Ultra System with monochromatic Al Kα X-rays (1486.71 eV) operated at 15 kV and 15 mA (emission current) in a chamber pressure of approximately 10^{-8} Pa. Energy step 1 and 160 eV pass energy were used for survey scan; energy step 0.1 and 20 eV pass energy were used for element scan.

The reducibility of the catalysts was measured with fixed-bed reactor. About 16 mg of 40–60 mesh catalyst was put in a U-shape reactor and kept at −15 °C for some time, then a gas stream of 5% H_2 in Ar was introduced into the reactor at a flow rate of 30 mL min^{-1}. H_2-TPR profile was recorded when the temperature was raised from −10 to 50 °C at a constant rate of 2 °C min^{-1}. The rate of hydrogen consumption during the reduction was monitored by a thermal conductivity detector (TCD).

Oxygen mobility of the catalysts was investigated using a temperature-programmed ^{18}O-isotope exchange method [22,30]. The measurements were carried out in a quartz reactor with an on-line-coupled quadruple mass spectrometer QMG421 I (Pfeiffer Vacuum GmbH). For each test, about 300 mg of catalyst was introduced into the reactor and pretreated at 450 °C for 4.5 h in air. After cooling down to 100 °C, a gas mixture of Ar, $^{16}O_2$, and $^{18}O_2$ with a pressure ratio of 4:1:1 and a total pressure of 100 Pa were introduced into the reaction system. All measurements were performed in the temperature range 100–700 °C with a heating rate of 10 °C min^{-1}. Between the gas phase $^{16}O_2$ and $^{18}O_2$ and the catalyst, several processes such as oxygen uptake/release, homogeneous gas phase ^{18}O-isotope exchange, partial heterogeneous ^{18}O-isotope exchange and complete heterogeneous ^{18}O-isotope exchange may take place separately or simultaneously depending on the nature of the compound and/or the temperature range investigated. The temperature dependence of the ionic currents (IC) of $^{16}O_2$, $^{18}O_2$, and $^{16}O^{18}O$ provide the information about the isotope exchange reaction. In order to differentiate between simultaneous processes, four different coefficients, *s*, *c*, *y* and *v*, are derived from the measured ionic currents [31–33]. *s* represents the oxygen partial pressure of the gas phase standardized by the oxygen partial pressure at the beginning of the measurement. It changes only when oxygen uptake/release occurs. *c* expresses the proportion of ^{18}O relative to the total oxygen content in the gas

phase. It decreases when oxygen is released, and partial or complete heterogeneous exchange processes take place. *y* describes the deviation of the actual partial pressure from the equilibrium partial pressure of the mixed isotope $^{16}O^{18}O$. A decrease in *y* shows the occurrence of the partial heterogeneous or homogeneous ^{18}O isotope exchange, while an increase in *y* indicates the release of $^{16}O_2$. *v* represents the fraction of ^{18}O in the gas phase that originates from the $^{16}O^{18}O$ molecules. It increases when any of the three types of ^{18}O isotope exchange processes takes place.

3. Results and discussion

3.1. Activity evaluation

The results of the catalytic tests for catalysts Pd/TiO_2–ZrO_2 are shown in Table 1. Pd/TiO_2 has the lowest activity. The addition of ZrO_2 enhances the catalytic activity for methane combustion; all Pd/TiO_2–ZrO_2 show higher activities than Pd/TiO_2. When atomic ratio of Zr:Ti is lower than 2:3, the activities of catalysts increase with the increasing content of ZrO_2, among which $T_{90\%}$ of the best catalyst Pd/TiZr2 is lower than that of Pd/TiO_2 more than 80 °C, even lower than that of Pd/ZrO_2, which is one of the most active catalysts for methane combustion. But when Zr:Ti > 2:3, the activities of Pd/TiO_2–ZrO_2 decrease, coming close to that of Pd/ZrO_2. In order to understand the behavior of different catalysts, XRD, XPS, TPR and ^{18}O-isotope exchange techniques were used to characterize selected catalysts.

3.2. XRD and XPS measurement

XRD was employed to identify the bulk phase compositions of all the catalysts. As shown in Fig. 1, Pd/TiO_2 and Pd/ZrO_2 display intensive and sharp peaks characteristic of anatase TiO_2 and monoclinic ZrO_2, respectively. XRD patterns of all the Pd/TiO_2–ZrO_2 catalysts have both the peaks of anatase TiO_2 and monoclinic ZrO_2 without any shift of peak positions, indicating that there is no interaction between TiO_2 and ZrO_2. The peak of PdO ($2\theta = 33.6°$) with the highest intensity is located at the same position with the peak of ZrO_2, so the characteristic peaks of PdO cannot be found in the XRD patterns of catalysts containing ZrO_2. From the XRD pattern of Pd/TiO_2, it can be seen that palladium exists in the state of PdO.

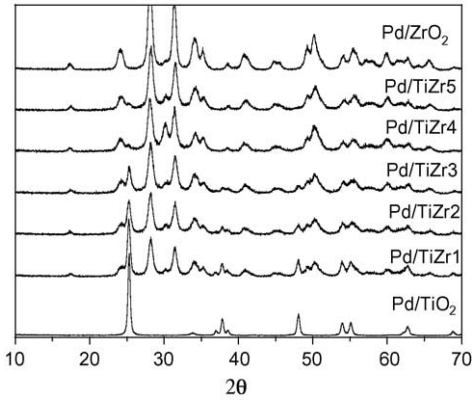

Fig. 1. The XRD patterns of all the catalysts.

The specific surface area and surface atom ratio of all catalysts are listed in Table 1. As is well known, surface atom ratio is closely related to the dispersion. The greater the surface atom ratio, the higher the dispersion. In the literatures, there are some confused reports about the relationship of the palladium dispersion and the activity of catalyst. Fujimoto et al. [8] and Muller et al. [36] reported a higher activity of larger PdO particles, but Widjaja et al. [37,38] demonstrated that the excellent activity of Pd/Al_2O_3–36NiO was due to the improved dispersion of PdO. Different from these opinions, our previous paper [22] suggested that the dispersion of palladium had little effect on the activity. The results herein approve the conclusion. For example, Pd/ZrO_2 has the highest surface ratio of Pd, but its activity is not the best; while the activity of Pd/TiZr1 is close to Pd/ZrO_2, but the surface Pd ratios of the two samples differ greatly. Therefore, it seems that the dispersion of palladium is not the decisive factor of the activity, which means the characters of supports and the metal–support interaction must be taken into account in this reaction.

3.3. H_2-TPR measurements

The reducibility of supported palladium oxide is an important factor influencing its catalytic performance [22].

Table 1
The BET surface areas, surface atom ratio and activity of different catalysts

Catalyst	Atom ratio (Ti:Zr)	BET surface area/$m^2\ g^{-1}$	Temperature/°C			Surface atom ratio			
			$T_{10\%}$	$T_{50\%}$	$T_{90\%}$	Pd	Ti	Zr	O
Pd/TiO_2		38.0	326	392	493	0.91	33.1		66.0
Pd/TiZr1	4:1	55.3	303	356	421	2.11	27.3	5.4	65.2
Pd/TiZr2	3:2	69.2	298	351	405	3.56	19.4	9.72	67.3
Pd/TiZr3	1:1	99.3	303	359	419	1.81	13.3	19.1	65.8
Pd/TiZr4	2:3	98.4	304	362	427	1.46	21.4	10.4	66.8
Pd/TiZr5	1:4	75.2	306	363	426	1.70	26.5	3.86	67.9
Pd/ZrO_2		55.0	299	358	420	3.97		29.0	67.0

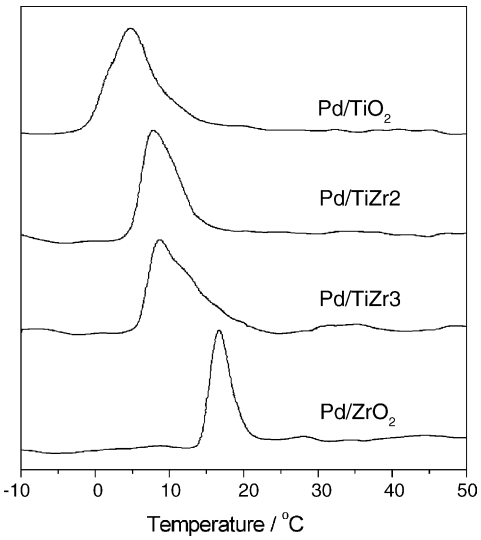

Fig. 2. The H_2-TPR patterns of the selective catalysts.

Temperature-programmed reduction technique was used to study the reducibility of catalysts. The TPR profiles of catalysts are shown in Fig. 2. For all samples investigated, there is a large peak below 30 °C corresponding to the reduction of PdO. To be noted, the supports themselves show no reduction peak in this temperature range. The reduction temperatures of the Pd/TiO_2–ZrO_2 catalysts are ranged from 5 °C of Pd/TiO_2 to 17 °C of Pd/ZrO_2, and the PdO reduction peaks

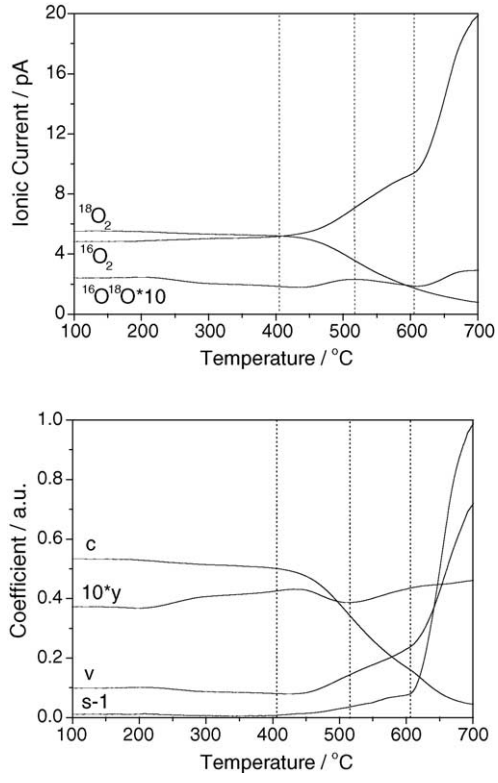

Fig. 3. Ionic current curves of $^{16}O_2$, $^{16}O^{18}O$ and $^{18}O_2$ and variations of the coefficients for catalyst Pd/TiZr2.

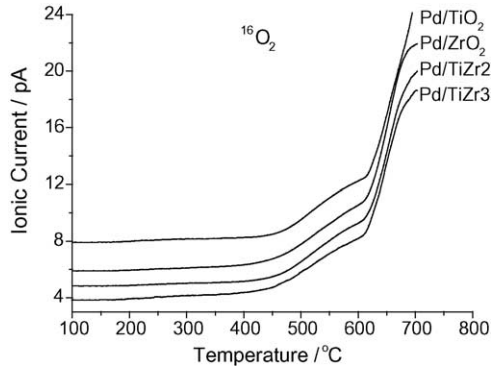

Fig. 4. Ionic current curves of $^{16}O_2$ for the selective catalysts.

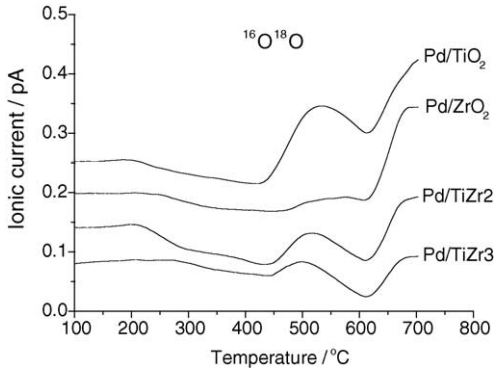

Fig. 5. Ionic current curves of $^{16}O^{18}O$ for the selective catalysts.

shift to the lower temperature side with the increasing content of titania.

3.4. Temperature-programmed ^{18}O-isotope exchange

Oxygen isotope exchange is a common method to study the uptake/release properties of oxygen and the participation of oxygen from the catalyst in oxidation reactions [22,30–35]. Temperature-programmed ^{18}O-isotope exchange measurements were carried out to investigate the oxygen mobility of selected catalysts. The samples selected are Pd/TiZr2 with the highest activity for methane combustion;

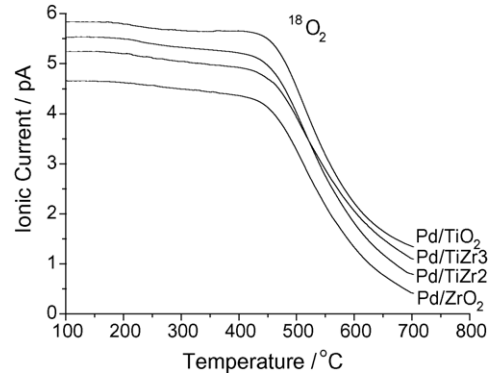

Fig. 6. Ionic current curves of $^{18}O_2$ for the selective catalysts.

Table 2
Temperature of $^{18}O_2$ isotope exchange and oxygen release processes for selected catalysts

Catalysts	Temperature range/°C		
	PHE[a] and R[b]; PHE[a] dominates over R[b]	CHE[c], R[b] and PHE[a], CHE[c] and R[b] predominate over PHE[a]	PHE[a], R[b] and CHE[c]; more PHE[a] and R[b]
Pd/TiO_2	426–532	532–615	615–700
Pd/TiZr2	405–517	517–606	606–700
Pd/TiZr3	415–500	500–613	613–700
Pd/ZrO_2	413–572	572–615	615–700

[a] Partial heterogeneous isotope exchange.
[b] Oxygen release.
[c] Complete heterogeneous isotope exchange.

Pd/TiZr3 and Pd supported on the single oxide Pd/TiO_2 and Pd/ZrO_2.

The results of ^{18}O-isotope exchange and the temperature dependence of the four coefficients of Pd/TiZr2 are presented in Fig. 3. When the temperature is below 405 °C, all the ionic currents of $^{16}O_2$, $^{18}O_2$, and $^{16}O^{18}O$ as well as the four coefficients are constant. At above 405 °C, $^{18}O_2$ begins to decrease and continues up to 700 °C. At the same time, the $^{16}O_2$ and the coefficients, *s* and *v*, increase with temperature from 405 to 700 °C, while the coefficient *c* decreases. But the rates of increase or decrease are different dependent on the temperature range. The *y* coefficient first decreases with reaction temperature demonstrating partial heterogeneous isotope exchange and reaches a minimum at 517 °C, and then it increases. When the temperature exceeds 606 °C, oxygen releases at a much higher rate, indicating the bulk decomposition of palladium oxide.

According to the variation of the ionic currents and the coefficients, the reaction process can be divided into three regions. The first region, between 405 and 517 °C, a decrease in $^{18}O_2$ ionic current is accompanied by increasing $^{16}O^{18}O$ and $^{16}O_2$ ionic currents. The coefficients *v* and *s* increase, while coefficients *c* and *y* decrease. From these results, it can be deduced that both partial heterogeneous isotope exchange (PHE) and oxygen release take place in this temperature range, PHE predominating over the oxygen release. In the second region 517–606 °C, $^{18}O_2$ and $^{16}O_2$ remain decreasing and increasing, respectively, while $^{16}O^{18}O$ turns to go down after reaching a maximum. The corresponding coefficients, s, *v*, and *c*, show variations similar to those in the first region, but *y* changes to increase. Complete heterogeneous isotope exchange (CHE), desorption and partial heterogeneous isotope exchange (PHE) take place in this temperature range, with CHE and desorption predominating over PHE. In the third region, between 606 and 700 °C, $^{18}O_2$ continues to decrease with a rapid increase in $^{16}O_2$, and $^{16}O^{18}O$ also increases. The coefficients *v* and *s* also increase at a much higher rate than in the first and second regions. The decrease in coefficient *c* slows down, and the coefficient *y* increases slowly. Therefore, PHE and oxygen release as predominant process take place at an increased rate in this temperature range, CHE occurs simultaneously.

Similarly, the four coefficients of other samples can be obtained from the ionic currents of $^{16}O_2$, $^{18}O_2$, and $^{16}O^{18}O$ (Figs. 4–6). Compared with Pd/TiZr2, they show more or less the same behavior in isotope exchange reaction, except for different temperature regions. The processes taking place on each sample during temperature programmed ^{18}O-isotope exchange measurements are summarized in Table 2.

Pd/TiZr2 displays the lowest onset temperature for ^{18}O-isotope exchange, indicating the highest oxygen mobility. The oxygen mobility of Pd/TiO_2 is the lowest, while Pd/ZrO_2 and Pd/TiZr3 have moderate oxygen mobility.

Our previous paper proved that the reducibility and oxygen-exchange activity of PdO were two factors directly related to the overall catalytic activity of palladium catalysts. A moderate reducibility and high oxygen mobility will lead to high methane conversion activity. The reducibility of Pd/TiZr2 is between that of Pd/TiO_2 and Pd/ZrO_2, but its oxygen mobility is much higher. Therefore, Pd/TiZr2 shows excellent catalytic activity for methane combustion at low temperature. Although Pd/ZrO_2 shows higher oxygen mobility than Pd/TiZr3, its lowest reducibility is an unfavorable factor in catalytic methane combustion. Therefore, Pd/ZrO_2 and Pd/TiZr3 have close catalytic activity for methane combustion. Pd/TiO_2 has highest reducibility and lowest oxygen mobility, both of which are harmful to methane combustion and lead to its lowest activity for methane combustion.

4. Conclusions

Catalysts of Pd supported on TiO_2–ZrO_2 binary oxides show very high activity for methane total oxidation at low temperature. Among them, Pd/TiZr2 with the highest activity shows a $T_{90\%}$ of 405 °C at a gas hourly mass velocity (GHMV) of 33,000 mL h^{-1} g^{-1}. It is about 80 °C lower than that of Pd/TiO_2, and even lower than that of Pd/ZrO_2 which is one of the catalysts with highest activity for methane total oxidation at low temperature.

The ^{18}O-isotope exchange measurements demonstrated that both partial and complete heterogeneous exchanges, as well as oxygen release, were observed for the selected catalysts. Compared with Pd/TiO_2 and Pd/ZrO_2, Pd/TiZr2 has

higher activity for oxygen exchange reaction and lower temperature for bulk palladium oxide decomposition. The excellent activity of Pd/TiZr2 is due to its high oxygen mobility and moderate reducibility. XPS results indicate that the dispersion of Pd has little influence on the catalytic activity.

Acknowledgments

We gratefully acknowledge the financial support from The Major State Basic Research Development Program (Grant No. G2000077503), National Science Foundation of China (20173002) and Cooperation project between NSFC and DFG (20411130104).

References

[1] E.S. Rubin, R.N. Cooper, R.A. Frosch, T.H. Lee, G. Marland, A.H. Rosenfield, D.D. Stine, Science 257 (1992) 148.
[2] M.M. Zwinkel, S.G. Jaras, P.C. Menon, Catal. Rev. Sci. Eng. 35 (1993) 319.
[3] L. Kundakovic, M. Flytzani-Stephanopoulos, Appl. Catal. A 183 (1999) 35.
[4] W.S. Epling, G.B. Hoflund, J. Catal. 182 (1999) 5.
[5] P. Gelin, M. Primet, Appl. Catal. B 39 (2002) 1.
[6] D. Ciuparu, M. Lyubovsky, E. Altman, L. Pfefferle, A. Datye, Catal. Rev. 44 (2002) 593.
[7] C.A. Muller, M. Maciejewski, R.A. Koeppel, A. Baiker, J. Catal. 166 (1997) 36.
[8] K. Fujimoto, F.H. Ribeiro, M. Avalos-Borja, E. Iglesia, J. Catal. 179 (1998) 431.
[9] J.N. Carstens, S.C. Su, A.T. Bell, J. Catal. 176 (1998) 136.
[10] K. Narui, K. Furuta, H. Yata, A. Nishida, Y. Kohtoku, T. Matsuzaki, Catal. Today 45 (1998) 173.
[11] C.A. Muller, M. Maciejewski, R.A. Koeppel, A. Baiker, Catal. Today 47 (1999) 245.
[12] W.S. Epling, G.B. Hoflund, J. Catal. 182 (1999) 5.
[13] S. Yang, A. Maroto-Valiente, M. Benito-Gonzalez, I. Rodriguez-Ramos, A. Guerro-Ruiz, Appl. Catal. B 28 (2000) 223.
[14] G. Groppi, Catal. Today 77 (2003) 335.
[15] M.A. Fraga, E. Soares de Souza, F. Villain, L.G. Appel, Appl. Catal. A 259 (2004) 57.
[16] J. Au-Yeung, K. Chen, A.T. Bell, E. Iglesia, J. Catal. 188 (1999) 132.
[17] D. Ciuparu, L. Pfefferle, Appl. Catal. A 209 (2001) 415.
[18] D. Ciuparu, E. Altman, L. Pfefferle, J. Catal. 203 (2001) 64.
[19] D. Ciuparu, L. Pfefferle, Catal. Today 77 (2002) 167.
[20] D. Ciuparu, F. Boaon-Verduraz, L. Pfefferle, J. Phys. Chem. B 106 (2002) 3434.
[21] G. Centi, J. Mol. Catal. A 173 (2001) 287.
[22] W. Lin, Y.X. Zhu, N.Z. Wu, Y.C. Xie, I. Murwani, E. Kemnitz, Appl. Catal. B 50 (2004) 59.
[23] C. Shi, L. Yang, Z. Wang, X. He, J. Cai, Chem. Commun. 18 (2002) 2006.
[24] C. Shi, L. Yang, Z. Wang, X. He, J. Cai, G. Li, X. Wang, Appl. Catal. A 243 (2003) 379.
[25] Y. Ozawa, Y. Tochihara, A. Watanbe, M. Nagai, S. Omi, Appl. Catal. A 258 (2004) 261.
[26] C.A. Müller, R.A. Koeppel, M. Maciejewski, J. Heveling, A. Baiker, Appl. Catal. A 145 (1996) 335.
[27] C. Bozo, N. Guilhaume, J.-M. Herrmann, J. Catal. 203 (2001) 393.
[28] T.-G. Kang, J.-H. Kim, S.G. Kang, G. Seo, Catal. Today 59 (2000) 87.
[29] C.-B. Wang, C.-M. Ho, H.-K. Lin, H.-C. Chiu, Fuel 81 (2002) 1883.
[30] Y.X. Zhu, I. Murwani, C.J. Zhou, E. Kemnitz, Y.C. Xie, Catal. Lett. 85 (2003) 205.
[31] E. Kemnitz, D.H. Menz, C. Stoecker, T. Olesch, Thermochim. Acta 225 (1993) 119.
[32] E. Kemnitz, A.A. Galkin, T. Olesch, S. Scheurell, A.P. Mozhaev, G.N. Mazo, J. Therm. Anal. 48 (1997) 997.
[33] I.K. Murwani, S. Scheurell, M. Feist, E. Kemnitz, J. Therm. Anal. Calorim. 69 (2002) 9.
[34] A. Hdmgren, D. Duprez, B. Andersson, J. Catal. 182 (1999) 441.
[35] M.K. Dongare, K. Malshe, C.S. Gopinath, I.K. Murwani, E. Kemnitz, J. Catal. 222 (2004) 80.
[36] C.A. Muller, M. Maciejewski, R.A. Koeprel, A. Baiker, Catal. Today 47 (1999) 245.
[37] H. Widjaja, K. Sekizawa, K. Eguchi, H. Arai, Catal. Today 35 (1997) 197.
[38] H. Widjaja, K. Sekizawa, K. Eguchi, H. Arai, Catal. Today 47 (1999) 95.